Sustainable Energy & Fuels

ROYAL SOCIETY OF CHEMISTRY

PAPER

View Article Online
View Journal | View Issue

Cite this: *Sustainable Energy Fuels*, 2021, **5**, 4311

Synthesis of tailored oxymethylene ether (OME) fuels *via* transacetalization reactions†

Marius Drexler, Philipp Haltenort, Thomas A. Zevaco, Ulrich Arnold * and Jörg Sauer

In the field of alternative diesel fuels, so-called oxymethylene ethers (OMEs) are currently intensely investigated. Particularly OMEs of the type $CH_3O(CH_2O)_nCH_3$ with n = 3–5 exhibit promising fuel properties and combustion characteristics with strongly reduced particle and NO_x emissions. According to their molecular structure, OMEs can be produced from methanol thus enabling sustainable production strategies from CO_2 and renewable resources. Compared to the methyl derivatives, analogous compounds with higher alkyl groups (oxymethylene dialkyl ethers, OMDAEs) have been investigated to a much lesser extent. Thus, commercially available OMDAEs, *i.e.* compounds of the type $ROCH_2OR$ bearing ethyl, propyl, butyl and 2-ethylhexyl groups, have been studied. Furthermore, asymmetric compounds of the type $R^1OCH_2OR^2$ have been synthesized from the symmetric compounds employing transacetalization reactions catalyzed by zeolite BEA-25. The OMDAEs have been characterized by spectroscopic and spectrometric methods and several physico-chemical, thermodynamic and fuel-related data have been determined and compared. Despite their structural peculiarities, such as the oxygen-containing acetal moiety in the molecular backbone, all OMDAEs exhibit properties similar to conventional diesel fuels. Based on experimental and analytical data, the development of tools for the prediction of properties by a simple regression method is described. Furthermore, the suitability of group contribution modelling is investigated for OMDAE compounds.

Received 23rd April 2021
Accepted 23rd July 2021

DOI: 10.1039/d1se00631b

rsc.li/sustainable-energy

Introduction

Oxymethylene ethers (OMEs) are currently attracting considerable interest due to their fuel properties and low emissions formed during the combustion process. In particular, oxymethylene dimethyl ethers (OMDMEs) are considered as a promising blending component for diesel fuels.[1,2] OMDMEs of the structure $CH_3O(CH_2O)_nCH_3$ with n = 3–5 exhibit properties similar to conventional diesel fuel and can be produced from renewable resources *via* methanol according to several synthesis pathways.[3–7] Thus, sustainable production with low overall emissions is possible.[8,9] Due to the absence of carbon–carbon bonds in the molecular structure, formation of particulate matter during combustion is inhibited to a large extent. This enables a higher rate of exhaust gas recirculation to reduce NO_x emissions as well.[10–14] To employ a synthetic fuel as drop-in fuel compatible with existing vehicles as well as infrastructures, it is inevitable to fulfil the respective diesel specifications, *e.g.* the EN 590 standard. Since many synthetic fuels do not meet all the specifications for fossil diesel fuel, an appropriate work-up and/or additives can be necessary to tune fuel properties.

In the case of OMEs, transacetalization reactions have recently been proposed to modify their structures and to adjust fuel properties.[15] The reactions proceed readily in the presence of acidic catalysts as outlined in Scheme 1. Thus, not only chain lengths can be varied but also the end groups and a series of oxymethylene dialkyl ethers (OMDAEs) bearing various alkyl groups become accessible. Such transacetalization reactions are a useful addition to the well-known acetalization reactions used for the production of OMEs from alcohols, especially methanol, and formaldehyde sources.[3,4,16–18]

Regarding low molecular weight OMDAEs with n = 1, *i.e.* dialkoxymethanes of the type $ROCH_2OR$, numerous representatives are known and some of them are commercially available, *e.g.* the derivatives with R = methyl, ethyl, propyl, butyl and 2-ethylhexyl. Dimethoxymethane (DMM, methylal, $OMDME_1$) is the most known compound in this series and it is used predominantly as a solvent.[19–21] Fuel properties of DMM have

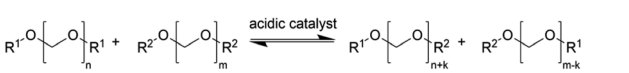

Scheme 1 General reaction scheme for transacetalization reactions of OMDAEs.

Karlsruhe Institute of Technology (KIT), Institute of Catalysis Research and Technology (IKFT), Hermann-von-Helmholtz-Platz 1, 76344 Eggenstein-Leopoldshafen, Germany. E-mail: ulrich.arnold@kit.edu

† Electronic supplementary information (ESI) available: Reaction monitoring, NMR-, FTIR- and mass spectra as well as tables with reference data. See DOI: 10.1039/d1se00631b

been investigated extensively and engine tests have been carried out.[22–25] It is also used for the synthesis of higher molecular weight OMEs, *e.g.* by chain extension reactions with formaldehyde sources like trioxane.[26–28] Regarding diethoxymethane (DEM) and dibutoxymethane (DBM), a series of physico-chemical data as well as fuel properties are available.[29–31] Compared to DMM, their use as fuels has been investigated to a much lesser extent.

As already stated above, transacetalization reactions of OMDAEs can easily be performed employing acidic catalysts and according to Scheme 1, asymmetric OMDAEs of the type $R^1(OCH_2)OR^2$ can be prepared *via* exchange of end groups. Some examples of such compounds are already known, *e.g.* methoxyethoxymethane (R^1 = methyl, R^2 = ethyl).[15] Regarding branched OMDAEs, the synthesis of methoxymethyl ethers for the protection of hydroxyl ethers has been described. In 2008, the preparation of (2-ethylhexyloxy)methoxymethane ((2-EH)MM) from 2-ethylhexanol and DMM has been reported.[32] Another example is the homologous (2-ethylhexyloxy)ethoxymethane ((2-EH)EM). In 1981, synthesis of (2-EH)EM by reaction of 2-ethylhexanol with DEM has been described.[33] In 2003, a patent on the production of ethoxymethyl ethers was filed which comprises the same reaction.[34] More recent studies report on the preparation of methoxymethyl ethers from alcohols by electrochemical methoxymethylation.[35] Furthermore, systematic investigations on physico-chemical properties, including various OMDAE compounds, have been published recently.[36,37]

Within this work, symmetric as well as asymmetric OMDAEs have been investigated with a strong focus on physico-chemical and fuel properties. Regarding the symmetric compounds, diethoxymethane (DEM), dipropoxymethane (DPM), dibutoxymethane (DBM) and di(2-ethylhexyloxy)methane (D(2-EH)M) have been purchased and extensively characterized. Furthermore, a series of asymmetric compounds has been synthesized by transacetalization reactions of D(2-EH)M with DEM, DPM and DBM, respectively. In previous work, zeolite BEA-25 proved to be a suitable acidic catalyst for such reactions and therefore, it has been chosen for this study.[15] The new compounds (2-ethylhexyloxy)propoxymethane ((2-EH)PM) and (2-ethylhexyloxy)butoxymethane ((2-EH)BM) have been characterized comprehensively and compared to the other derivatives.

Furthermore, physico-chemical and fuel properties of the OMDAEs are compared to OMDMEs and alkanes with similar chain length. In this context, two methods for the prediction of structure-related properties are suggested, a simple regression technique and a thermodynamic group-contribution approach. The methods can support the design of tailor-made OMDAEs and the adjustment of properties according to the respective requirements.

Methods

Materials

Diethoxymethane (DEM, ≥99%) was purchased from Merck KGaA while dipropoxymethane (DPM, ≥99%) and dibutoxymethane (DBM, ≥99%) were obtained from Lambiotte & Cie. Di(2-ethylhexyloxy)methane (D(2-EH)M, 95%) was purchased from Chemos GmbH & Co. KG. All chemicals were used without further purification. Zeolite BEA-25 (CP814E*) was provided by Zeolyst International. Prior to use, it was calcined for 5 h at 500 °C and dried for 12 h at 110 °C under reduced pressure.

Synthesis of OMDAEs

The reactions have been carried out in a glass flask equipped with a condensation cooler. An oil bath has been used for heating and the reaction mixtures have been stirred magnetically at 400 rpm. Experiments with dipropoxymethane (DPM)

Table 1 Labelling, molecular structure, CAS number, molar mass and oxygen content of the investigated OMDAEs

Compound (abbreviation)	Molecular structure	CAS no.	Molar mass g mol^{-1}	Oxygen content wt%
Diethoxymethane (DEM)		462-95-3	104.15	30.72
Dipropoxymethane (DPM)		505-84-0	132.20	24.21
Dibutoxymethane (DBM)	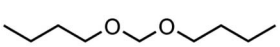	2568-90-3	160.26	19.97
Di(2-ethylhexyloxy)methane (D(2-EH)M)	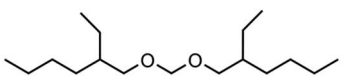	22174-70-5	272.47	11.74
(2-Ethylhexyloxy)ethoxymethane ((2-EH)EM)	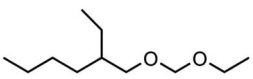	80390-85-8	188.31	16.99
(2-Ethylhexyloxy)propoxymethane ((2-EH)PM)	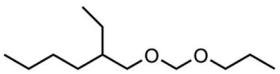	—	202.34	15.81
(2-Ethylhexyloxy)butoxymethane ((2-EH)BM)	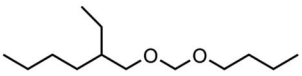	—	216.37	14.79

and dibutoxymethane (DBM) have been carried out at 80 °C while a reaction temperature of 60 °C has been chosen in the case of diethoxymethane (DEM). The zeolite catalyst BEA-25 has been fixed in a stainless steel basket, which has been placed in the middle of the flask.

In each experiment 10 g of catalyst (0.78 wt%) were employed and equimolar amounts of the educts have been used. The reactions have been monitored by continuous sampling from the reaction mixtures. After reaction, the mixtures were cooled down to room temperature and filtrated. All investigated compounds, the commercially available ones as well as the synthesized compounds, are summarized in Table 1.

Characterization of products

The composition of the liquid samples as well as the purity of the products have been determined by gas chromatography employing a Hewlett Packard 6890 Series FID gas chromatograph equipped with a DB-5 column from Agilent. Helium has been used as a carrier gas.

NMR spectra were recorded on a Varian Inova 400 instrument employing concentrated benzene D6 (deuteration grade 99.8%) solutions. FTIR spectra have been recorded in transmittance mode on a Varian IR-FT Carry 660 instrument employing thin films between KBr plates. The measuring range was from 250 to 4000 cm^{-1} with 8 scans per measurement and a resolution of 1 cm^{-1}. The spectra were edited using "Spectragryph – optical spectroscopy software".[38] Mass spectra of the samples were recorded with an Agilent 5973 mass spectrometer coupled with an Agilent 6890N GC system.

Densities of the compounds have been measured at 20 °C using a DMA 4500 M density meter from Anton Paar. Dynamic viscosities have been determined with a Modular Compact Rheometer model MCR 102 from Anton Paar. The measurements have been carried out at 20 °C with a concentric cylinder system. Melting points have been determined by DSC measurements with a Netzsch DSC214 Polyma. The samples were cooled down to −150 °C and subsequently heated to −50 °C with a rate of 5 K min^{-1}. Phase transitions have been determined by observation of changes in the required heating power. Regarding heat of combustion (ΔH_c^0), a C5000 calorimeter from IKA has been employed. With these data, heat of formation (ΔH_f^0) as well as lower and higher heating values of the compounds have been calculated. Additionally, the indicated cetane number (ICN, EN 17155), flash point (ASTM D 7094), lubricity (high frequency reciprocating rig test HFRR, EN ISO 12156-1), cold behavior (cold filter plugging point CFPP, EN 116), auto ignition temperature (DIN 51794), surface tension (EN 14370), refractive index (DIN 51423-2) and distillation characteristics (EN 17306) have been determined by ASG Analytik-Service AG (Neusäss, Germany) according to certified standard methods.

Prediction of physico-chemical and fuel properties

Transacetalization reactions (Scheme 1) enable the synthesis of versatile OMDAE compounds. Even if oligomeric products ($R^1O(CH_2O)_nR^2$ with $n > 1$) are neglected, the combination of different end groups leads to various species. Some of these products might show well-suited properties for a technical use as fuels, solvents or reactants. Therefore, the estimation of properties, based on molecular structures, is highly desirable for OMADEs. Current models for the prediction of physical properties and especially fuel properties are very sophisticated, relying on large databases and complex calculation methods.[36,37,39–47] A common type of predictive model described in literature is the group contribution method. It describes the investigated compound as a set of molecular groups. Within this approach, physico-chemical properties are calculated solely based on molecular structure. In the case of transacetalization reactions such a model, for instance the Joback method, appears to be applicable.[48] As a simple exchange of end groups between the OMDAEs is conducted, the modification of number and nature of the molecular groups is clearly defined.

Therefore, the standard Joback method has been employed and a comparison of predicted and measured properties of OMDAEs has been carried out. The method has been used in its original form without any modification of the groups or the contribution parameters. Detailed information on this procedure is provided in the ESI (Tables E5 and E6†). Since acetal groups are not implemented in the standard Joback method, a combination of a CH_2-group and two bridging oxygen atoms has been used to mimic this structure. To extend the experimental database, additional data for similar compounds taken from the literature have been included. Since the acetal structure is implemented by a simple mimic approach, deviations between measured and predicted values are to be expected. As a result, insights on structure related systematic errors for the prediction of the group contribution method can be gained. These findings can be relevant for future work with a focus on the development of prediction techniques for OMDAEs. Several authors have provided tailored versions of the Joback method in the field of fuel research to estimate physico-chemical properties and fuel data.[49–51] The conclusions of this study might encourage the development of suitable methods for OMDAEs as well.

The discussion of systematic errors considers the known uncertainties of the prediction method. Therefore, the relative average errors stated for the original Joback method[48] have been adapted. For the enthalpy of formation (ΔH_f^0) the average absolute error of 8.4 kJ mol^{-1} is employed.[48] The deviations between the predicted and measured values will be expressed by mean absolute errors (MAE). This leads to a more individual context for the investigated properties.

In contrast to the application of the group contribution method, a simple prediction approach by a regression according to eqn (1) has been employed.

$$y = a_0 + a_1 M + a_2 e^{-\frac{M}{a_3}} \quad (1)$$

By fitting the coefficients a_n it becomes possible to appropriately describe correlations between molecular properties of structurally similar OMDAEs, especially in terms of molar masses M, and their physico-chemical as well as fuel properties. The set of values used to fit the coefficients was obtained from

the reactants DEM, DPM, DBM and D(2-EH)M as well as from literature data for DMM and dipentoxymethane (DPeM) which is provided in the ESI (Tables E7 and E8†). This method, also called *ad hoc* descriptor approach can provide a reasonable prediction with little effort.[52] It is less sophisticated compared to other methods, as the prediction relies on few structural properties and therefore its versatility is limited. In the case of transacetalization reactions as conducted in this work, this limitation is acceptable since structures of the compounds are similar.[53] Examples of linear or exponential correlations to predict properties of organic compounds employing molar mass, number of carbon atoms or other input parameters can be found in literature.[52,54–56]

Results and discussion

Synthesis of asymmetric OMDAEs

For the synthesis of asymmetric OMDAEs, the symmetric D(2-EH)M bearing 2-ethylhexyl groups has been reacted with the symmetric DEM, DPM and DBM, respectively. Zeolite BEA-25 has been used as catalyst. The reaction progress has been monitored and time-dependent molar compositions of the reaction mixtures have been recorded. Exemplary results for the reaction of D(2-EH)M with DBM are shown in Fig. 1. During reaction, no significant formation of side products has been observed and after reaction, the mixture contained approximately equal amounts of the educts D(2-EH)M and DBM amounting to about 25 mol%, respectively. The content of the desired asymmetric (2-EH)BM was about 50 mol%. It was separated from the reaction mixture by distillation under reduced pressure and further purified by distillation until purity was above 99% with respect to GC-Area. The procedure for the preparation of the related (2-EH)EM and (2-EH)PM was essentially the same and detailed information is given in the ESI in section A.†

Characterization of asymmetric OMDAEs

The structure of the compounds could be clearly assessed *via* ^{1}H and ^{13}C NMR spectroscopy due to the high purity of the samples

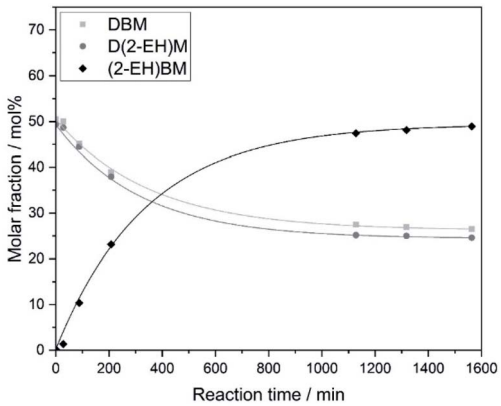

Fig. 1 Transacetalization reaction of D(2-EH)M with DBM catalyzed by zeolite BEA-25 (reaction conditions: 80 °C, 400 rpm, 0.78 wt% catalyst).

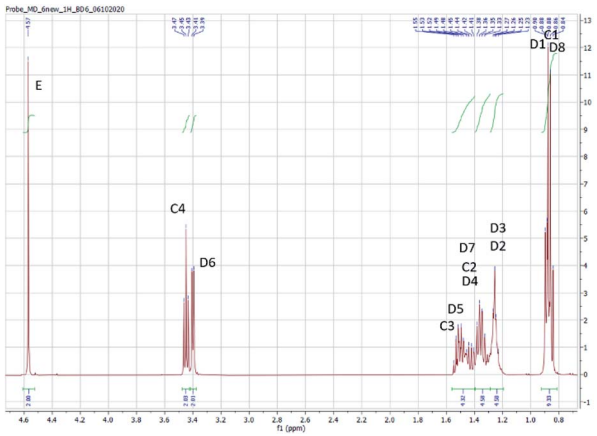

Fig. 2 ^{1}H NMR spectrum of (2-EH)BM: δ (ppm, in benzene-d6).

and a general good solubility in benzene-d6. The assignment of the numerous NMR-signals found for the OMDAEs is customarily made correlating the information gained from dedicated 1D methods (*e.g.*, DEPT 135 and ^{13}C measured with gated decoupling) and standard 2D-NMR spectra, in this case ^{1}H,^{1}H COSY and ^{1}H,^{13}C HETCOR. The recorded chemical shifts and coupling patterns were compared to NMR data from the literature[33,57,58] and from the ^{1}H and ^{13}C prediction tools of ChemDraw 19 (part of the ChemOffice 2019 software package) and of ACD/C + H Predictors & DB 2019.1.1. (from the Software package ACD/Labs 2019.1.1). To avoid needless redundancy, typical 1D ^{1}H and ^{13}C spectra (Fig. 2 and 3) together with a 2D ^{13}C,^{1}H-correlated spectrum (Fig. 4) are depicted exemplarily for the asymmetric derivative (2-EH)BM in the following. The complete NMR-characterization of all the derivatives can be found in the ESI in section B.† The nomenclature to assign the signals is following the scheme shown in Scheme 2, with letters indicating the groups and numbers denoting the carbon atoms. It should be stated that, due to the similarity of the chemical environments of some methylene groups, a small ambiguity remains in the assignment of some signals (*e.g.* the carbon pairs D2,D7 and D3,D4 in the 2-ethylhexyloxy fragment whose chemical shifts might be swapped).

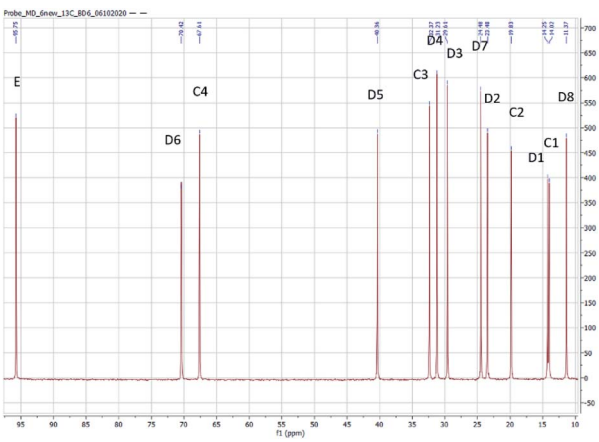

Fig. 3 ^{13}C NMR spectrum of (2-EH)BM: δ (ppm, in benzene-d6).

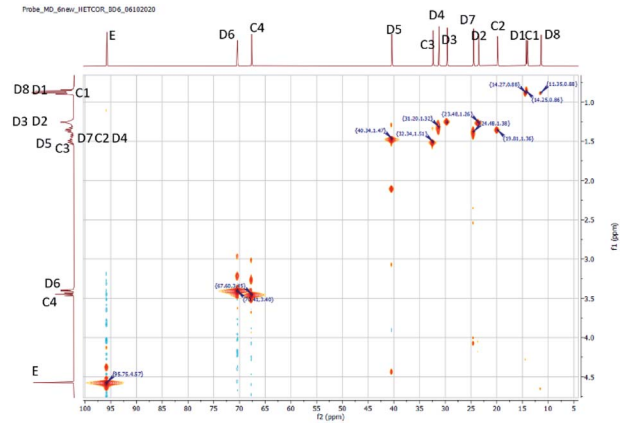

Fig. 4 $^{1}H,^{13}C$ HETCOR 2D spectrum of (2-EH)BM: δ (ppm, in benzene-d6).

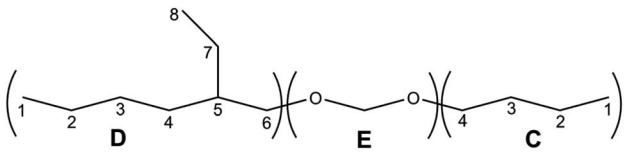

Scheme 2 Labelling for NMR analysis of (2-EH)BM.

The ^{1}H NMR spectra of the OMDAEs can be generally divided in four main regions typical of specific fragments: (1) the central methylene bridge found at low field (around 4.5 ppm), displaying no coupling pattern with other spin systems, (2) the methylene groups in alpha location of the oxygen atoms, in both alkyl groups attached to the oxymethylene pivot (located between 3.4 and 3.6 ppm – expressed either as triplet or doublet depending on their environment), (3) the methylene groups belonging to the bulk of the alkane chains with complex coupling patterns and signals ranging from 1.2 to 1.5 ppm, and (4) the methyl groups capping the alkane chains, found at around 0.8 ppm (Fig. 2).

The ^{13}C NMR spectra of the asymmetric OMDAEs can be roughly seen as a superposition of two ^{13}C signal sets of the parent symmetric OMDAEs. For instance, the asymmetric compound (2-EH)BM can be seen, through the NMR looking glass, as the combination of the ^{13}C spectra of the symmetric compounds D(2-EH)M and DBM (Fig. 3). Similarly to the ^{1}H spectra, the ^{13}C spectra of the OMDAEs can be divided in four main ranges related to specific fragments: (1) the central methylene bridge found at low field (around 95 ppm), (2) both methylene groups in alpha location of the oxymethylene pivot (located around 65–70 ppm), (3) the methylene groups belonging to the bulk of the alkyl groups ranging from 20 to 40 ppm, and (4) the methyl groups terminating the alkane chains found around 11–14 ppm. Interestingly, measuring the ^{13}C spectra in the "gated decoupling" mode allowed to gain some knowledge about the $^{1}J_{C-H}$ coupling constant: The central oxymethylene group displaying a high C–H coupling constant of *ca.* 160 Hz whereas the carbons in alpha location of this central group amount to 140 Hz and the bulk of the remaining methylene and methyl groups display more common $^{1}J_{C-H}$ coupling constants around 124 Hz.

The $^{1}H,^{13}C$ HETCOR spectrum complements nicely the former spectra, allowing an unambiguously attribution of the

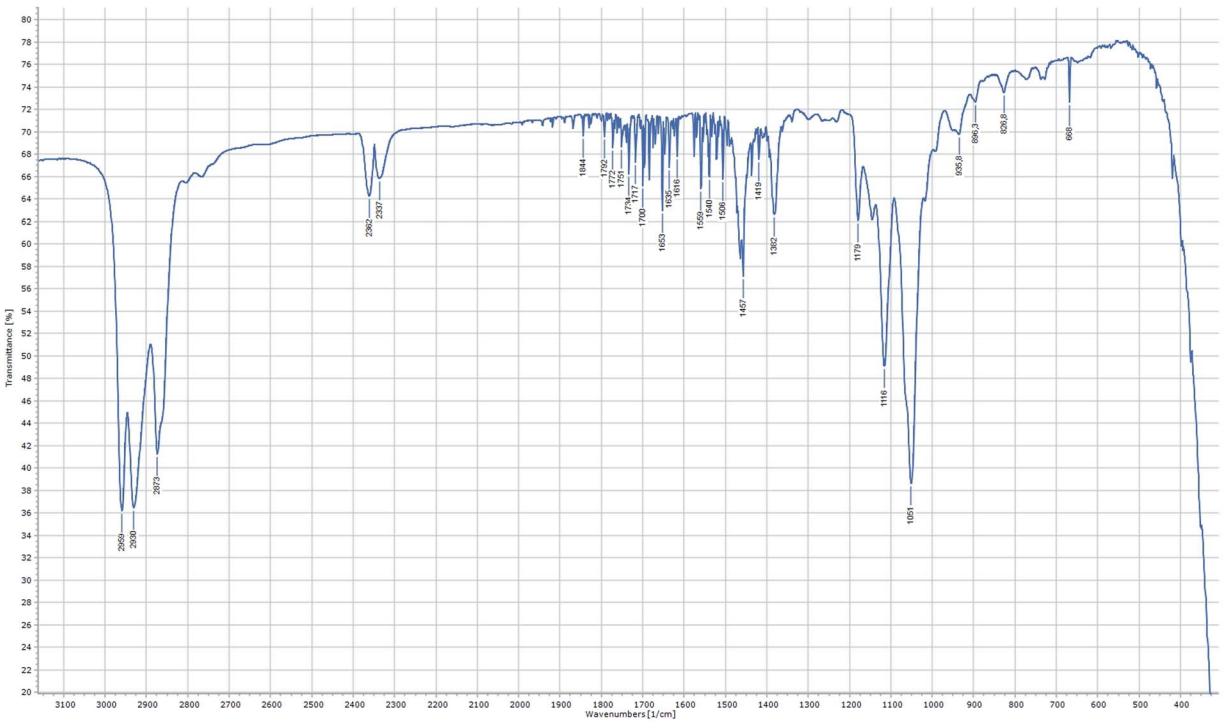

Fig. 5 FTIR spectrum of (2-EH)BM (recorded in transmittance mode as thin film between KBr plates, resolution 1 cm^{-1}, 8 scans).

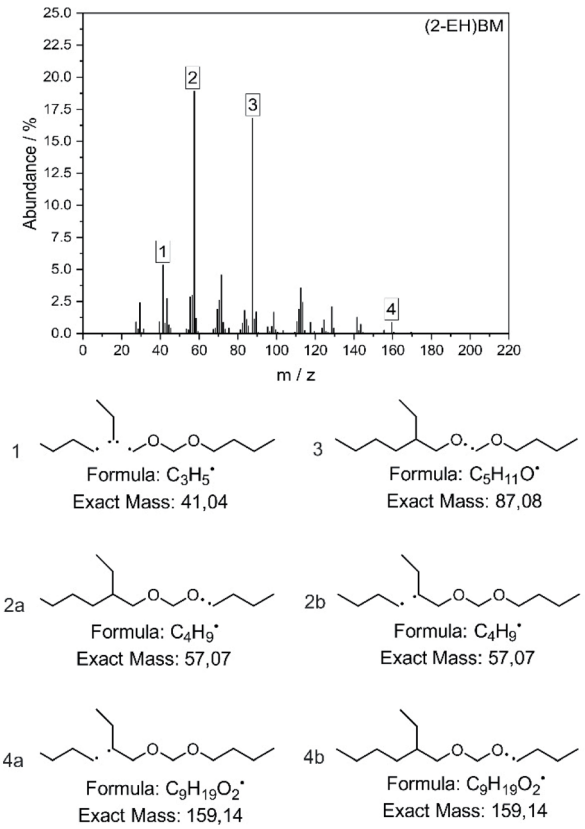

Fig. 6 Mass spectrum of (2-EH)BM and assignment of the relevant fragments.

numerous ^{13}C and ^{1}H NMR signals of the compound and clearly outlining the four signal regions mentioned above (Fig. 4).

Regarding the IR-spectra of the OMDAEs (recorded as thin films between KBr plates), the main absorption bands related to the C–H and C–O fragments can be easily localized (see Fig. 5).[59] The strong C–H stretching bands are found around 2870 cm^{-1} for the symmetric and between 2930 and 2970 cm^{-1} for the asymmetric ones, the bands belonging to the methyl group having usually a slightly higher frequency than those of the methylene groups. The characteristic C–O stretching bands are found between 900 and 1200 cm^{-1}: the asymmetric ones between 1040 and 1200 cm^{-1} being definitely stronger than the symmetric ones, measured around 800–900 cm^{-1}. Interestingly, whereas one strong ν(C–O) asymmetric band is commonly found in the spectra of "mono"-ethers, the OMDAEs display a more complex pattern in this characteristic region, probably due to the presence of two connected ether functions causing more complex vibration patterns. Complementing the strong stretching C–H vibrations, numerous deformation modi typical of the methylene fragment (scissoring, wagging and rocking, among others) can also be seen in the spectra: δ scissoring around 1460 cm^{-1}, wagging & twisting (ω & τ) around 1380 cm^{-1} and rocking (ρ) in the 800–950 cm^{-1} region. The complete FTIR-characterization of all the derivatives can be found in the ESI in section C.†

The molecular structure of the compounds has also been verified by mass spectrometry and the spectrum for (2-EH)BM is shown in Fig. 6. The most important fragments are identified and shown in the figure. Spectra recorded for the other products can be found in the ESI in section D.†

The fragments with the highest abundance are found to be $C_4H_9^{\bullet}$ **2** and $C_5H_{11}O^{\bullet}$ **3**. Fragments of the type $C_4H_9^{\bullet}$ can result from two mechanisms for this product, represented by **2a** and **2b**. Especially compounds comprising butyl end groups show clear peaks in this position, since they are able to access both fragmentation mechanisms. The corresponding fragments of the type $C_9H_{19}O_2^{\bullet}$ can be found at **4**, but only to a small amount since further fragmentation to $C_3H_5^{\bullet}$ or $C_5H_{11}O^{\bullet}$ as shown in **1** and **3** is likely. Comparison of the spectra to those of compounds with a similar structure *e.g.* 2-ethylhexanol[60,61] or DBM[62] confirm the suggested fragmentation mechanism.

Physico-chemical properties

The physico-chemical properties of the compounds are displayed in Table 2. Properties of comparable *n*-alkanes as well as OMDMEs are summarized in Table E2.† The influence of the molecular structure on physico-chemical and fuel properties of OMDAEs can be studied by comparing the different OMDAEs among each other and by comparing them to the corresponding OMDMEs and n-alkanes with similar molar mass. Regarding density, a clear correlation with the molar mass is observed for each substance class (Fig. 7). OMDMEs exhibit significantly higher densities than the corresponding OMDAEs while densities of the n-alkanes are the lowest.

Table 2 Physico-chemical properties of OMDAEs

Compound	Density at 20 °C, kg m^{-3}	Molar volume, cm^3 mol^{-1}	Melting point, °C	Boiling point, °C	Refractive index
DEM	829.7	125.5	−66.6	87.1	1.373
DPM	834.6	158.4	−98.7	135.2	1.393
DBM	835.4	191.8	−59.5	178.8	1.406
D(2-EH)M	848.2	321.2	−120.6	285.1	1.435
(2-EH)EM	842.7	223.5	−134.3	205.8	1.418
(2-EH)PM	843.3	239.9	−135.4	221.9	1.421
(2-EH)BM	843.2	256.6	−132.3	237.6	1.424
Diesel (EN 590)	820–845[a]	—	−20[b]–0	180–340	—

[a] At 15 °C. [b] CFPP of winter diesel.

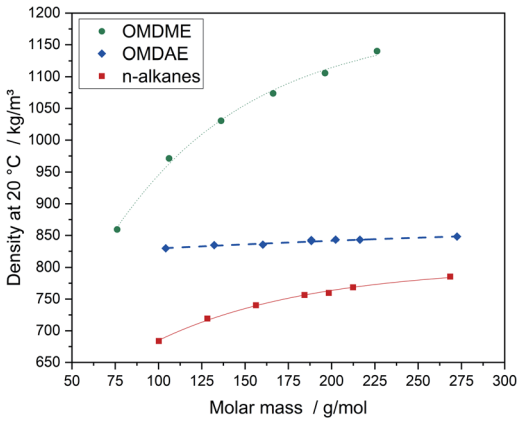

Fig. 7 Densities of OMDAEs compared to OMDMEs and *n*-alkanes with similar molar mass. Data points and trend lines for OMDMEs (green) and *n*-alkanes (red) as well as data points and values predicted by the regression function for OMDAEs (blue).

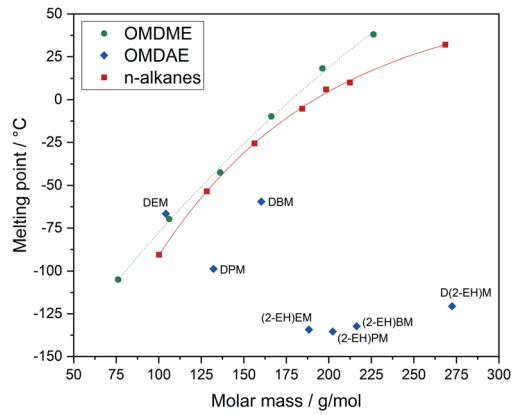

Fig. 8 Melting points of OMDAEs compared to OMDMEs and *n*-alkanes with similar molar mass. Data points and trend lines for OMDMEs (green) and *n*-alkanes (red) as well as data points for OMDAEs (blue).

The higher density of the oxygenate compounds can be explained by stronger intermolecular forces caused by oxygen, which results in a higher packing density. The remarkably higher densities of OMDMEs compared to OMDAEs, are most likely due to their higher oxygen content. It should be noted, that densities of the OMDAEs slightly increase with increasing molar mass and remain in a comparatively narrow range between 829 and 849 kg m^{-3}. Fitting of the values of the OMDAEs with the regression function mentioned above, as indicated by the bold dashed line in Fig. 7, results in a very good correlation with molar mass.

The melting points of the OMDAEs are within a broad range from −59 to −136 °C (Fig. 8). Compared to values for *n*-alkanes and OMDMEs from the literature an opposite trend is observed. The melting points for alkanes increase with increasing molar mass due to stronger van-der-Waals forces. The values for branched OMDAEs on the other hand decrease despite increasing molar mass, which might be due to the structural

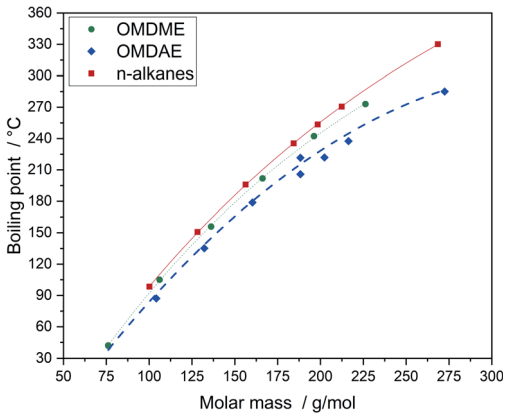

Fig. 9 Boiling points of OMDAEs compared to OMDMEs and *n*-alkanes with similar molar mass. Data points and trend lines for OMDMEs (green) and *n*-alkanes (red) as well as data points and values predicted by the regression function for OMDAEs.

properties of the molecules. Regarding alkanes, it is well known that the melting point of a compound depends on the packing density of the molecules, enabling stronger van-der-Waals forces and therefore causing higher melting points.[63] The packaging density on the other hand is depending on the physical structure of the molecule, *e.g.* symmetry or branching. This leads to lower melting points for compounds with a more complex or irregular molecular structure. Since the structures of OMDAEs are generally more irregular than those of *n*-alkanes and OMDMEs, the packing density and consequently the melting points are lower. This effect is particularly pronounced in the case of branched compounds which becomes obvious, for example, by comparing linear and branched alkanes.[63] Regarding OMDAEs, the lowest melting points are observed in the case of derivatives bearing the branched 2-ethylhexyl group.

The boiling points of the compounds can be correlated very well with the molar mass (Fig. 9). The increasing values come along with increasing molar mass which is due to increasing intermolecular attractive forces.[63] Compared to *n*-alkanes or OMDMEs the branched OMDAE compounds exhibit significantly lower boiling points with respect to their molar mass, which might be due to structural characteristics. Branching prevents optimum proximity of the molecules to each other, reducing the intermolecular forces and thus the boiling point, which is also observed in the case of alkanes.[63]

As expected, a linear relationship between density and refractive index can be observed within the group of symmetric compounds and within the group of asymmetric compounds. Like in the case of density, the values for the refractive index increase with increasing molar mass.

Regarding the physico-chemical properties discussed so far, all branched OMDAEs synthesized within this work fulfil the requirements according to the EN 590 standard. The extremely low melting points might be an interesting feature regarding the potential of the compounds as fuel additives. By comparison, the cold stability of pure OMDME fuels is much more limited. In addition, except for melting points, all synthesized

Table 3 Fuel properties of OMDAEs

Compound	Cetane number	Autoignition point, °C	Flash point, °C	Kinematic viscosity at 20 °C, $mm^2 s^{-1}$	HFRR, µm	CFPP, °C	Surface tension, $mN m^{-1}$
DEM	41.4	170	−5.0	0.52	760	<−60	21.0
DPM	51.5	255	29.5	0.85	690	−52	23.1
DBM	74.6	185	60.5	1.22	780	<−60	24.3
D(2-EH)M	75.6	205	133.5	4.56	420	−32	27.1
(2-EH)EM	63.8	185	80.5	1.58	790	< −60	24.7
(2-EH)PM	69.6	190	91.5	1.98	510	−37	24.6
(2-EH)BM	79.0	195	103.0	2.32	610	−49	25.6
Diesel (EN 590)	>51	~220	>55	2.0–4.5[a]	<460	<−20[b]	26

[a] At 40 °C. [b] Winter diesel.

compounds exhibit physico-chemical characteristics with values between those of the corresponding educts. This might allow for a rough estimation of several properties.

Fuel properties

To estimate the suitability of OMDAEs for fuel applications, several fuel properties have been determined (Table 3). Furthermore, fuel properties of OMDAEs are compared to those of OMDMEs, *n*-alkanes and conventional diesel fuel (EN 590). Detailed data for all substance classes are known and can be found in Table E3.†

One of the most important parameters for diesel fuels is the cetane number, which is inversely associated with the fuels ignition delay.[64] Since the ignition behaviour of a fuel is determined by the kinetics of initial radical formation governed by complex interaction of local conditions in the engine, it is very difficult to predict. The cetane number on the other hand is a reliable parameter to evaluate suitability of a compound or blend for applications as a diesel fuel. For commercial diesel fuels, a cetane number of 51 or higher is required, according to the EN 590 standard. The cetane numbers of the investigated OMDAEs as well as the cetane numbers of comparable OMDMEs and *n*-alkanes are shown in Fig. 10. While OMDMEs and *n*-alkanes show an almost linear relation between molar mass and cetane number, there is no apparent trend for the OMDAEs. While the general trend of increasing cetane number with increasing molar mass is still recognizable, there seems to be a correlation between branching and cetane number. In general, branching in the alkyl groups seems to decrease the cetane number of the compound. A possible explanation can be found in a study of Han *et al.*, which focuses on the autoignition characteristics of different fuel classes.[65] According to this study, the cetane number or ignition delay strongly depends on the formation of radicals in the initial steps of the ignition process, which leads to chain branching reactions. In the case of branched alkanes and ethers it is argued, that there is a higher number of primary carbon atoms exhibiting a higher bonding energy and thus hindering H transfer. Furthermore, the branches lead to steric hindrance and impede the formation of transition rings. This causes not only a deformation of transition rings, which enhances the activation energy of isomerization reactions but also reduces the probability of capturing H atoms by O atoms. Despite these effects, it is noticeable that all synthesized compounds exceed by far the minimum cetane number of 51 defined by EN 590. Thus, the compounds represent interesting cetane enhancers for diesel fuels.

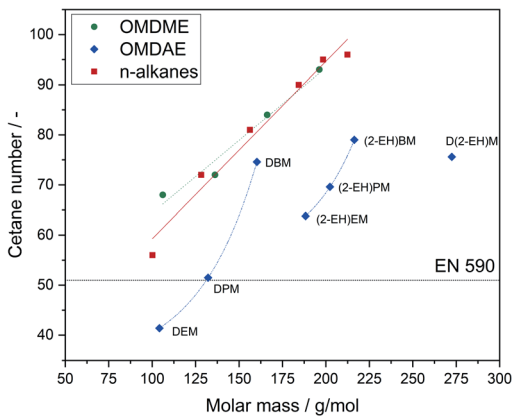

Fig. 10 Cetane numbers of OMDAEs compared to OMDMEs and *n*-alkanes with similar molar mass. Data points and trend lines for OMDMEs (green), *n*-alkanes (red) and OMDAEs (blue).

Other important fuel properties regarding ignition behaviour are the autoignition point and the flash point. The autoignition point is determined by the temperature resulting in spontaneous ignition of the fuel in mixture with air. The autoignition points for the compounds synthesized within this work are in the range of 185 to 195 °C and therefore lower than the values for *n*-alkanes with similar molar mass (202–220 °C) and also lower than the values for OMDMEs (230–240 °C). In general, the values of the asymmetric branched OMDAEs lie in between those of their symmetric educts, with the exception of DPM, which exhibits a remarkably high autoignition temperature.

The flash point describes the lowest temperature at atmospheric pressure enabling the formation of a flammable vapour–air mixture in a closed container. It correlates strongly with the boiling point. If the boiling points of the educts are known, this connection can be used to design compounds and to adjust flash points according to the respective requirements.

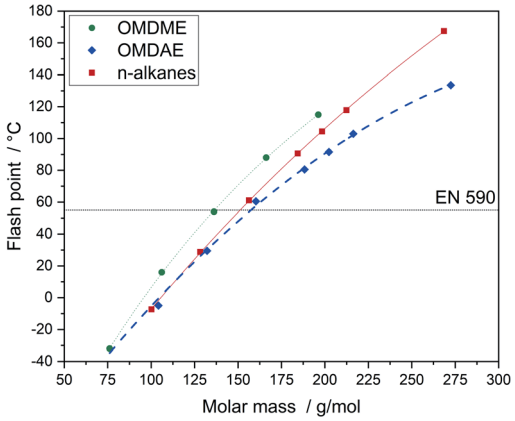

Fig. 11 Flash points of OMDAEs compared to OMDMEs and *n*-alkanes with similar molar mass. Data points and trend lines for OMDMEs (green) and *n*-alkanes (red) as well as data points and values predicted by the regression function for OMDAEs (blue).

The flash point is a critical parameter regarding safety and it plays a key role with respect to infrastructural issues like fuel storage and transportation.[64] Flash points of OMDAEs, OMDMEs and *n*-alkanes as a function of molar mass are depicted in Fig. 11. The flash points of OMDAEs as well as OMDMEs and *n*-alkanes show a strong correlation with the molar mass of the components, with OMDAEs exhibiting the lowest and OMDMEs the highest values with respect to their molar mass. All flash points of the synthesized compounds are in the range of 80 to 103 °C and therefore in the required range above 55 °C.

The viscosity is an important parameter for fuel injection and spray formation in the combustion chamber. Too high values can cause problems regarding fuel pumping as well as cold start while too low values can cause problems during hot start and increase wear of the fuel pump.[64] According to EN 590, viscosity should be in the range of 2.0 to 4.5 $mm^2 s^{-1}$ at 40 °C. Thus, optimum injection and droplet formation is ensured. Comparing OMDAEs to OMDMEs and *n*-alkanes, OMDAEs exhibit the lowest while *n*-alkanes exhibit the highest values (Fig. 12). For kinematic viscosity, the same phenomenon as in the case of boiling points can be observed. Due to lower packing densities caused by the molecular structure, intermolecular forces of OMDAEs are lower compared to OMDMEs and *n*-alkanes. Obviously, the impact of the oxygen content is relatively weak compared to steric effects. Consequently, the branched molecules exhibit lower viscosities compared to the corresponding OMDMEs and *n*-alkanes. Within each substance class, kinematic viscosity increases exponentially with increasing molar mass.

Another relevant fuel property is the lubricity, which is usually determined by the high frequency reciprocating rig (HFRR) method. The lubricity of a fuel is essential since the moving parts of modern fuel injection pumps are lubricated by the fuel itself.[66] With exception of D(2-EH)M, the HFRR values of OMDAEs are higher than the corresponding values of OMDMEs as well as the required value for diesel fuel. This might be due to the lower oxygen content compared to OMDMEs, since lubricity of the compounds is strongly influenced by the presence of oxygen in the molecular structure.[67] The low HFRR value of D(2-EH)M might be due to its branched molecular structure. Previous studies with oxygenated fuels already demonstrated the successful use of lubricity improvers in the case of DBM without affecting the engine performance.[30]

The cold behaviour of a fuel is usually described by the cold filter plugging point (CFPP). It depicts the lowest temperature at which the fuel is filterable. According to EN 590, it should be below −20 °C for fuel used in winter. Due to the CFFP value being strongly connected to the freezing point of a substance, this limit is surpassed by each OMDAE investigated within this work (Table 3).

Regarding fuel injection, surface tension is another important parameter. If the surface tension is too high, the formation of droplets during injection is hindered resulting in incomplete combustion and therefore higher emissions of air pollutants. Fig. 13 summarizes the values determined for OMDAEs,

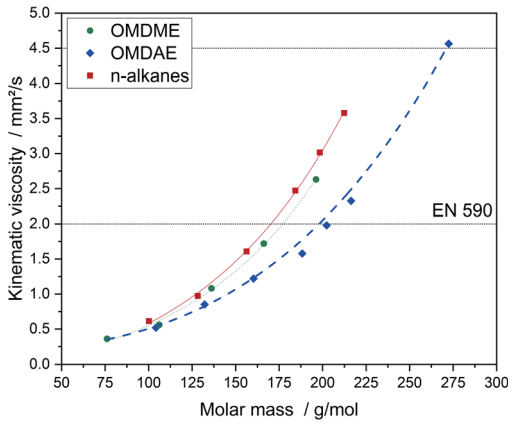

Fig. 12 Kinematic viscosity of OMDAEs compared to OMDMEs and *n*-alkanes with similar molar mass. Data points and trend lines for OMDMEs (green) and *n*-alkanes (red) as well as data points and values predicted by the regression function for OMDAEs (blue).

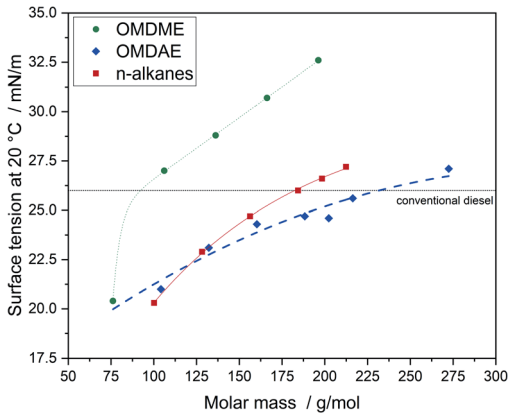

Fig. 13 Surface tension of OMDAEs compared to OMDMEs and *n*-alkanes with similar molar mass. Data points and trend lines for OMDMEs (green) and *n*-alkanes (red) as well as data points and values predicted by the regression function for OMDAEs (blue).

Table 4 Thermodynamic properties of OMDAEs

Compound	ΔH_f^0, kJ mol^{-1}	ΔH_c^0, kJ mol^{-1}	LHV, MJ kg^{-1}	HHV, MJ kg^{-1}
DEM	−566.44	3115.86	27.38	29.92
DPM	−543.06	4497.84	31.36	34.02
DBM	−549.21	5850.29	33.76	36.51
D(2-EH)M	−749.55	11084.35	37.77	40.68
(2-EH)EM	−585.56	7172.54	35.29	38.09
(2-EH)PM	−632.34	7805.06	35.75	38.57
(2-EH)BM	−641.70	8475.00	36.32	39.17
Diesel (EN 590)	—	—	42.6	45.4

OMDMEs and *n*-alkanes. OMDMEs exhibit higher values for surface tension than *n*-alkanes of comparable molar mass, probably due to increased intermolecular forces caused by the oxygen content. The values for the branched OMDAEs are significantly lower than those of the *n*-alkanes. This seems to be following the trend observed in the case of kinematic viscosity, *i.e.* branching is decisive and the influence of the oxygen content is much lower compared to branching. It should be noted, that for oxygenated compounds the droplet formation is not as decisive regarding the formation of air pollutants as for hydrocarbons, as the oxygen demand required for complete combustion is reduced by the oxygen content of the molecule. This effect has already been demonstrated in studies reducing the pressure of the fuel injection system.[68]

Regarding their use as a fuel, the branched OMDAEs synthesized within this work exhibit some promising properties. Especially their good cold behavior indicated by very low CFPP values might be used to improve the stability of oxygenated fuels such as OMDMEs. In the same context, the high flash points of several OMDAEs are an interesting feature to improve the safety and reduce the complexity of storage and transportation of such fuels. Both, CFPP as well as flash points, have been shown to be critical properties, limiting the share of certain fractions of OMDME fuels.[69] By adding tailored OMDAEs, it might be possible to circumvent restrictions regarding fuel compositions, enabling simplified and therefore economical production of such fuels.

Thermodynamic properties

Some thermodynamic properties of the compounds are listed in Table 4 and discussed in the following. Detailed data for all substance classes are known and can be found in Table E4.† The higher heating values (HHV) as well as the lower heating values (LHV) of OMDAEs and OMDMEs are remarkably lower compared to *n*-alkanes of similar molar mass (Fig. 14). The values are directly related to the oxygen content and OMDMEs exhibit the lowest values. The oxygen content of OMDMEs is in the range of 42 to 49 wt% and increases with increasing chain length while the LHV decreases. In contrast, the oxygen content of OMDAEs decreases from 31 to 12 wt% with increasing chain length and the LHV increases. Following the oxygen content, the values are closer to OMDMEs for short chain molecules and approximate those of the *n*-alkanes with increasing chain length.

Regarding their use as fuels, the reduced heating values and heat of combustion lead to an increase in fuel consumption. For OMDMEs it was reported, that the volume of fuel injected into the engine in each stroke needs to be increased by 70 to 80 vol% compared to diesel fuel. This could be achieved by minor modification of engine components, *e.g.* enlargement of the injection nozzle diameter as well as adjustments in the engine control.[68] However, OMDAEs enable the access on fuel compounds with heating values between OMDMEs and conventional diesel fuels. Thus, blending could enhance the LHV of OMDME fuels without a significant decrease of the overall oxygen content. Otherwise, OMDAEs could increase the oxygen content of conventional diesel fuels with a decent decrease of the LHV. This strategy appears interesting, as even small oxygen contents lead to significant reduction of smoke in exhaust gases.[70]

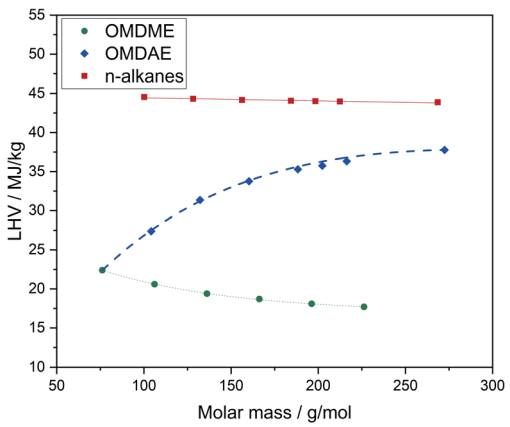

Fig. 14 Lower heating values of OMDAEs compared to OMDMEs and *n*-alkanes with similar molar mass. Data points and trend lines for OMDMEs (green) and *n*-alkanes (red) as well as data points and values predicted by the regression function for OMDAEs (blue).

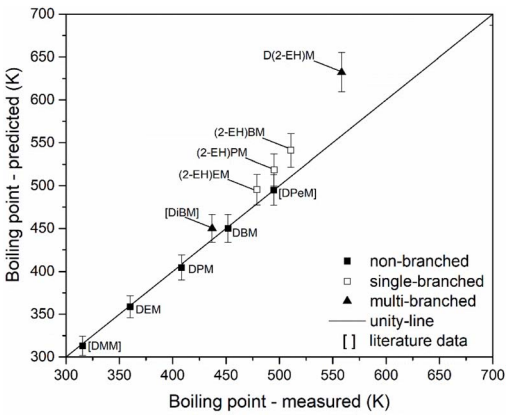

Fig. 15 Parity plot of measured and predicted boiling points of OMDAEs. Prediction based on the Joback group contribution method. Experimentally measured data points from the literature are labelled in brackets.

Prediction of physico-chemical and fuel properties

The suitability of group contribution models for the prediction of some key properties of OMDAEs has been evaluated employing the Joback method. Parity analyses have been carried out to compare experimental and predicted physico-chemical data and to evaluate the quality of such models. If available, literature information has been employed to extend the data set. This enables a stronger indication of findings, due to an increased database. To clearly distinguish between the measurements conducted in this study and the data points from literature, the latter ones are labelled in square brackets in the following parity plots.

Fig. 15 shows a parity plot for the boiling points of OMDAEs. The graph is based on data from this work and already published data for DMM, di(isobutoxy)methane (DiBM) and DPeM.[71] There is an excellent prediction of boiling points for the non-branched OMDAEs (MAE = 2 K) while the single-branched OMDAEs show notable errors (MAE = 23 K). Considering the uncertainties of the Joback method, (2-EH)EM might match the unity-line, but for (2-EH)PM and (2-EH)BM the deviation of measured and predicted values appears to be significant. The multi-branched compounds DiBM and D(2-EH)M show elevated differences between the measured and estimated boiling points (MAE = 44 K). While estimation errors could explain the observed deviation of DiBM, the significant error for D(2-EH)M might be due to a systematic overprediction.

Regarding dynamic viscosity, the investigated compounds DEM, DPM and DBM show a good parity between estimated and predicted values (Fig. 16). Analysis of the non-branched OMDAEs was extended by data for DMM from Zheng *et al.*[72] Interestingly, DMM shows a significant deviation between the experimental and the estimated value. However, the total difference for DMM (0.1 mPa s) is quite small and does not affect the overall good parity of the non-branched OMDAEs (MAE = 0.07 mPa s). The single-branched compounds exhibit an overprediction of dynamic viscosity (MAE = 0.12 mPa s). Due to the increased errors determined by Joback and Reid,[48] these observations are still within the systematic errors of the estimation method. A comparable situation could be identified for D(2-EH)M. The multi-branched compound shows an absolute error of 0.45 mPa s.

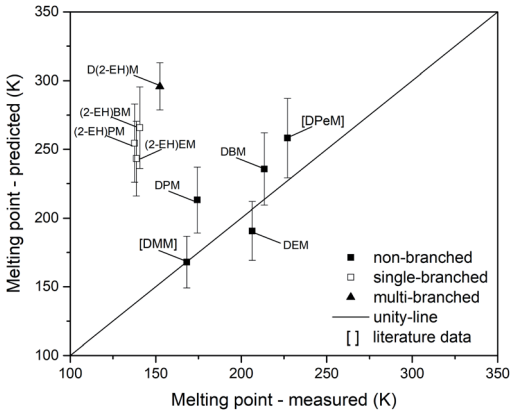

Fig. 17 Parity plot of measured and predicted melting points of OMDAEs. Prediction based on the Joback group contribution method. Experimentally measured data points from the literature are labelled in brackets.

The parity analysis for melting points is shown in Fig. 17. Literature data points for DMM[73] and DPeM[71] have been added for this analysis. If prediction errors are considered, a suitable prediction might be possible for DMM, DEM and DBM. Noteworthy, the non-branched compounds DPM and DPeM do not match the parity-line for the melting point. Furthermore, significant deviations could be found for the single-branched (MAE = 116 K) and multi-branched (MAE = 143 K) compounds. Considering the mean error for the non-branched OMDAEs (MAE = 22 K), additional branching of the side chains leads to increasing errors. Besides this structural finding, the overall predictive precision of melting points appears unsatisfyingly, except for DMM.

The last property used for the evaluation of group contribution modelling of OMDAEs is ΔH_f^0. The data set has been

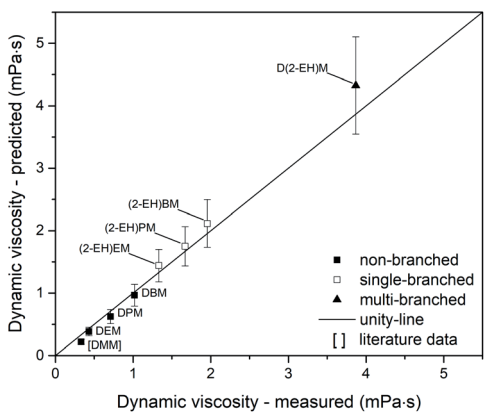

Fig. 16 Parity plot of measured and predicted dynamic viscosities of OMDAEs. Prediction based on the Joback group contribution method. Experimentally measured data points from the literature are labelled in brackets.

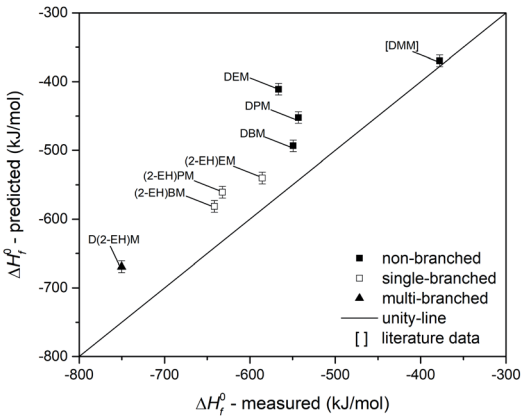

Fig. 18 Parity plot of measured and predicted values for the heat of formation ΔH_f^0 of OMDAEs. Prediction based on the Joback group contribution method. Experimentally measured data points from the literature are labelled in brackets.

extended with literature data for DMM[73] and is shown in Fig. 18. There is an excellent prediction for DMM, but regardless of their type of branching, all measured data of OMDAEs exhibit significant deviations. Apparently this is due to a systematic overprediction of the Joback method. The trend between the MAE and the branching of the OMDAEs could not be observed for ΔH_f^0. This finding might be due to the high error of DEM, which leads to an MAE of 77.5 kJ mol^{-1} for the non-branched compounds and does not result in trend with the MAE for single-branched (59.1 kJ mol^{-1}) and multi-branched (81.1 kJ mol^{-1}) compounds.

Comparison of predicted and measured data leads to findings, which can contribute to the further refinement of prediction techniques: first, the observed prediction accuracy is higher for non-branched compounds, except for ΔH_f^0. As external data for DMM and DPeM support this observation, this finding appears to be independent of systematic experimental errors. Second, the type of branching appears to influence the estimation accuracy. For all predicted properties with the exception of ΔH_f^0, the multi-branched compounds show higher errors compared to the single-branched OMDAEs. Third, the high accordance of the predictions for the non-branched OMDAEs leads to the conclusion that the substitution of the acetal group by a combination of a CH_2 unit and two bridging oxygen atoms does not negatively influence the property estimation of the boiling point, the dynamic viscosity and the melting point. For ΔH_f^0 there might be an effect of the acetal group in combination with side chains larger than methyl groups. This assumption is based on the observed overprediction in Fig. 18. This phenomenon should be assessed in future work with a focus on group contribution modelling for OMDAEs.

The investigated examples indicate that group contribution methods like the Joback method can be well-suited for the prediction of some OMDAE properties. For other properties, *e.g.* the melting point or ΔH_f^0, further studies are required to find suitable prediction models.

Employing the regression function (1) it has been found, that most of the physico-chemical and some fuel properties directly correlate with the molar mass of the OMDAE compounds. The coefficients used to fit the function as well as the coefficient of determination r^2 and the MAE indicating the fit quality are listed in Table 5. By using this empirical regression function, it is possible to accurately predict some properties of the compounds. It should be noted, that the correlation is only applicable to compounds similar to those used to fit the coefficients, in this case OMDAEs of the type $R^1O(CH_2O)_nR^2$ with $n = 1$. It should also be noted, that the introduction of branched groups can change some properties drastically, impeding a prediction based on values of the non-branched analogues. As a result, some properties such as melting points could not be predicted reliably. However, this problem might be overcome by extending the database, thus considering structurally more similar compounds as a basis for the prediction. While not as universal as a group contribution method, this approach enables efficient identification of compounds suitable for a specific application, starting from a database with scarce data points.

Both employed estimation techniques, the Joback method and the simple regression technique, could not predict all investigated properties precisely for all investigated compounds. Therefore, the employed modelling approaches should be enhanced, aiming at higher accuracy and including further physico-chemical data and fuel properties. With a larger data set at hand, it might be possible to refine the presented methods and take structural related characteristics into account as well. The influence of branching of the side chains and the acetal group should be considered in the design of future experimental data sets for OMDAEs. Furthermore, more sophisticated modelling strategies should be evaluated.

In the case of group contribution modelling strategies, considering intramolecular interactions could lead to a better prediction for branched species. Additionally, combinatorial effects of structural properties, like the branching of side chains in the presence of the acetal group, could be taken into account with these approaches.

Including larger datasets, could also be a suitable strategy to refine the regression technique according to eqn (1).

Table 5 Regression coefficients for properties of OMDAEs investigated within this work

	Coefficients[a]					MAE	
Property	Unit	a_0	a_1	a_2	a_3	r^2	Fitting error	Prediction error
Density	kg m^{-3}	2102.12	−0.50012	−1288.25	1917.27	0.98	0.76	1.38
Molar volume	cm^3 mol^{-1}	1.72	1.17685	1.00	1.00	1.00	1.54	0.16
Boiling point	°C	47 635.61	−17.00362	−47773.71	2434.93	1.00	3.44	8.60
Refractive index	—	1.55	-2.278×10^{-4}	−0.29	160.44	1.00	3.72×10^{-4}	6.80×10^{-4}
Flash point	°C	14 896.03	−6.74759	−15 041.46	1795.48	1.00	2.25	0.88
Kinematic viscosity	mm^2 s^{-1}	−1.35	−0.0112	1.57	−156.35	1.00	0.01	0.16
Surface tension	mN m^{-1}	983.63	−0.39987	−968.55	2041.72	0.98	0.26	0.58
ΔH_f^0	kJ mol^{-1}	−364.03	−1.38632	798.36	1.63	0.89	26.70	24.17
ΔH_c^0	kJ mol^{-1}	−1725.78	47.04603	1.00	1.00	1.00	26.68	24.02
LHV	MJ kg^{-1}	50.69	−0.03274	−53.23	105.24	1.00	0.07	0.45
HHV	MJ kg^{-1}	52.13	−0.02893	−53.88	100.37	1.00	0.07	0.44

[a] Based on molar mass M in g mol^{-1}.

Nevertheless, it could be assumed that this simple regression is not feasible to predict all relevant properties solely based on their molar mass. This appears appropriate *e.g.* in the context of the known dependency of the cetane number and the molecular structure of hydrocarbons.[74,75] Therefore, more versatile regression strategies might be required. By considering additional properties, refined mathematic expressions and an extended set of fitting parameters, modern strategies for the development of suitable prediction techniques could be employed. Therefore, recently demonstrated modelling approaches utilizing machine learning and neural networks show promising results and should be considered.[43,76,77]

Enhancing the quality and capability of the property prediction techniques could contribute to a predictive driven development of tailor-made compounds for fuel applications *via* transacetalization reactions. Furthermore, the prediction of physico-chemical properties allows a rapid integration of versatile OMDAE compounds in process development and scale-up. This drastically reduces the experimental and analytical efforts to identify interesting compounds in a field with a tremendous amount of different chemical species, thus reducing the associated development costs.

Conclusions

OMDAEs of the type $R^1OCH_2OR^2$ have been studied in terms of synthesis, structural characterization, physico-chemical and fuel properties. In general, OMDAEs can be produced by acetalization reactions of formaldehyde sources with alcohols. Since formaldehyde is usually obtained from methanol, production is logically based on methanol and higher alcohols. Thus, a sustainable production from renewable feedstocks is possible provided that the alcohols are obtained from renewables. Symmetric compounds with $R^1 = R^2$ as well as asymmetric compounds with $R^1 \neq R^2$ have been considered. Regarding the former ones, commercially available derivatives bearing ethyl, propyl, butyl and 2-ethylhexyl groups have been employed while the latter ones have been synthesized *via* transacetalization reactions of symmetric compounds catalyzed by zeolite BEA-25. Employing this approach, a series of OMDAEs with various end groups is easily accessible. In this context, two new asymmetric compounds have been prepared for the first time: the derivative with 2-ethylhexyl and propyl groups as well as the derivative with 2-ethylhexyl and butyl groups.

The compounds have been characterized in detail by NMR and FTIR spectroscopy as well as mass spectrometry. To assess the suitability for fuel applications, all OMDAEs have been analyzed with respect to numerous parameters ranging from physico-chemical data such as densities, melting or boiling points to important combustion characteristics such as cetane numbers, autoignition points or heating values. The obtained data are compared to corresponding data of OMDMEs ($R^1 = R^2 = CH_3$) and hydrocarbons with similar chain length and data are often in good accordance with the EN 590 standard for diesel fuel.

In many cases clear correlations between structure, especially molar mass, and properties become visible. Thus, structure–performance relationships can be derived, which allow for a targeted fuel design and synthesis. Based on experimental and analytical data obtained within this work a model for the prediction of several properties can be developed and two approaches, one by regression and another one by a group contribution method, are described. Consequently, it becomes possible to estimate values for similar compounds, offering a design strategy to develop new fuels with specific properties. The development of more precise estimation techniques, *e.g.* by extension of the standard Joback method, appears to be a promising tool for this approach. Based on our initial demonstration, the prediction of further properties should be investigated and used to expand the predictive capabilities for OMDAEs.

Current work concentrates on modification and optimization of OMDAEs. By reactions with alternative formaldehyde sources, *e.g.* trioxane, chain length can be extended by incorporation of additional CH_2O groups and oligomers of the type $R^1O(CH_2O)_nR^2$ with $n > 1$ can be synthesized. Furthermore, applications, *e.g.* as fuel additives and blending components, are investigated and, in the next step, engine tests will be carried out to evaluate their fuel performance.

Author contributions

M. Drexler: synthesis and purification of the compounds, formal analysis and visualization, original draft, review & editing. P. Haltenort: conceptual design for property estimation, group contribution modelling, review & editing. T.A. Zevaco: NMR measurements, NMR & IR attribution & contributing the related written parts. U. Arnold: funding acquisition, conceptualization, supervision, investigation, writing, reviewing & editing. J. Sauer: funding acquisition, supervision, reviewing & editing.

Conflicts of interest

There are no conflicts to declare.

Acknowledgements

The authors gratefully acknowledge financial support from the Bundesministerium für Bildung und Forschung (BMBF) within the NAMOSYN Project (FKZ 03SF0566K0). We also thank Zeolyst International for providing catalysts.

Notes and references

1 J. Burger, M. Siegert, E. Ströfer and H. Hasse, Poly(oxymethylene) dimethyl ethers as components of tailored diesel fuel: Properties, synthesis and purification concepts, *Fuel*, 2010, **89**, 3315–3319.
2 A. Omari, B. Heuser, S. Pischinger and C. Rüdinger, Potential of long-chain oxymethylene ether and oxymethylene ether-diesel blends for ultra-low emission engines, *Appl. Energy*, 2019, **239**, 1242–1249.

3 K. Hackbarth, P. Haltenort, U. Arnold and J. Sauer, Recent Progress in the Production, Application and Evaluation of Oxymethylene Ethers, *Chem. Ing. Tech.*, 2018, **90**, 99.
4 D. Oestreich, L. Lautenschütz, U. Arnold and J. Sauer, Reaction kinetics and equilibrium parameters for the production of oxymethylene dimethyl ethers (OME) from methanol and formaldehyde, *Chem. Eng. Sci.*, 2017, **163**, 92–104.
5 D. Deutsch, D. Oestreich, L. Lautenschütz, P. Haltenort, U. Arnold and J. Sauer, High Purity Oligomeric Oxymethylene Ethers as Diesel Fuels, *Chem. Ing. Tech.*, 2017, **89**, 486–489.
6 B. Niethammer, S. Wodarz, M. Betz, P. Haltenort, D. Oestreich, K. Hackbarth, U. Arnold, T. Otto and J. Sauer, Alternative Liquid Fuels from Renewable Resources, *Chem. Ing. Tech.*, 2018, **90**, 99–112.
7 A. Peter, H. Scherer, E. Jacob and I. Krossing, in *Internationaler Motorenkongress 2020*, ed. J. Liebl, C. Beidl and W. Maus, Springer Vieweg, Wiesbaden, 2020, pp. 405–414.
8 M. Ouda, G. Yarce, R. J. White, M. Hadrich, D. Himmel, A. Schaadt, H. Klein, E. Jacob and I. Krossing, Poly(oxymethylene) dimethyl ether synthesis – a combined chemical equilibrium investigation towards an increasingly efficient and potentially sustainable synthetic route, *React. Chem. Eng.*, 2017, **2**, 50–59.
9 R. Sun, C. Mebrahtu, J. P. Hofmann, D. Bongartz, J. Burre, C. H. Gierlich, P. J. C. Hausoul, A. Mitsos and R. Palkovits, Hydrogen-efficient non-oxidative transformation of methanol into dimethoxymethane over a tailored bifunctional Cu catalyst, *Sustainable Energy Fuels*, 2021, **5**, 117–126.
10 M. Härtl, P. Seidenspinner, G. Wachtmeister and E. Jacob, Synthetic Diesel Fuel OME1 A Pathway Out of the Soot-NOx Trade-Off, *MTZ Worldwide*, 2014, **75**, 48–53.
11 D. Pélerin, K. Gaukel, M. Härtl, E. Jacob and G. Wachtmeister, Potentials to simplify the engine system using the alternative diesel fuels oxymethylene ether OME1 and OME3−6 on a heavy-duty engine, *Fuel*, 2020, **259**, 1–10.
12 C. J. Baranowski, A. M. Bahmanpour, F. Héroguel, J. S. Luterbacher and O. Kröcher, Insights into the Nature of the Active Sites of Tin-Montmorillonite for the Synthesis of Polyoxymethylene Dimethyl Ethers (OME), *ChemCatChem*, 2019, **72**, 34.
13 C. J. Baranowski, A. M. Bahmanpour and O. Kröcher, Catalytic synthesis of polyoxymethylene dimethyl ethers (OME), *Appl. Catal., B*, 2017, **217**, 407–420.
14 A. Omari, B. Heuser and S. Pischinger, Potential of oxymethylenether-diesel blends for ultra-low emission engines, *Fuel*, 2017, **209**, 232–237.
15 P. Haltenort, L. Lautenschütz, U. Arnold and J. Sauer, (Trans) acetalization Reactions for the Synthesis of Oligomeric Oxymethylene Dialkyl Ethers Catalyzed by Zeolite BEA25, *Top. Catal.*, 2019, **62**, 551–559.
16 N. Schmitz, J. Burger and H. Hasse, Reaction Kinetics of the Formation of Poly(oxymethylene) Dimethyl Ethers from Formaldehyde and Methanol in Aqueous Solutions, *Ind. Eng. Chem. Res.*, 2015, **54**, 12553–12560.
17 Karlsruhe Institute of Technology, *European Union Pat.*, EP2987781B1, 2015.
18 A. Fink, C. H. Gierlich, I. Delidovich and R. Palkovits, Systematic Catalyst Screening of Zeolites with Various Frameworks and Si/Al Ratios to Identify Optimum Acid Strength in OME Synthesis, *ChemCatChem*, 2020, **12**, 5710–5719.
19 A. Zhenova, A. Pellis, R. A. Milescu, C. R. McElroy, R. J. White, J. H. Clark and J. H. Clark, Solvent Applications of Short-Chain Oxymethylene Dimethyl Ether Oligomers, *ACS Sustainable Chem. Eng.*, 2019, **7**, 14834–14840.
20 M. Schappals, T. Breug-Nissen, K. Langenbach, J. Burger and H. Hasse, Solubility of Carbon Dioxide in Poly(oxymethylene) Dimethyl Ethers, *J. Chem. Eng. Data*, 2017, **62**, 4027–4031.
21 L. Faba, E. Díaz and S. Ordóñez, Recent developments on the catalytic technologies for the transformation of biomass into biofuels: A patent survey, *Renewable Sustainable Energy Rev.*, 2015, **51**, 273–287.
22 *Chemistry of diesel fuels*, ed. C. Song, C. S. Hsu and I. Mochida, Taylor & Francis, New York, NY, 2000.
23 M. Härtl, P. Seidenspinner, E. Jacob and G. Wachtmeister, Oxygenate screening on a heavy-duty diesel engine and emission characteristics of highly oxygenated oxymethylene ether fuel, *Fuel*, 2015, **153**, 328–335.
24 M. Härtl, P. Seidenspinner, G. Wachtmeister and E. Jacob, Synthetischer Dieselkraftstoff OME1 — Lösungsansatz für den Zielkonflikt NOx-/Partikel-Emission, *Motortech. Z.*, 2014, **75**, 68–73.
25 K. D. Vertin, J. M. Ohi, D. W. Naegeli, K. H. Childress, G. P. Hagen, C. I. McCarthy, A. S. Cheng and R. W. Dibble, in *SAE Technical Paper Series*, SAE International400 Commonwealth Drive, Warrendale, PA, United States, 1999.
26 L. Lautenschütz, D. Oestreich, P. Haltenort, U. Arnold, E. Dinjus and J. Sauer, Efficient synthesis of oxymethylene dimethyl ethers (OME) from dimethoxymethane and trioxane over zeolites, *Fuel Process. Technol.*, 2017, **165**, 27–33.
27 R. Peláez, P. Marín and S. Ordóñez, Synthesis of poly(oxymethylene) dimethyl ethers from methylal and trioxane over acidic ion exchange resins: A kinetic study, *Chem. Eng. J.*, 2020, **396**, 125305.
28 J. Burger, E. Ströfer and H. Hasse, Chemical Equilibrium and Reaction Kinetics of the Heterogeneously Catalyzed Formation of Poly(oxymethylene) Dimethyl Ethers from Methylal and Trioxane, *Ind. Eng. Chem. Res.*, 2012, **51**, 12751–12761.
29 L. Lautenschütz, D. Oestreich, P. Seidenspinner, U. Arnold, E. Dinjus and J. Sauer, Physico-chemical properties and fuel characteristics of oxymethylene dialkyl ethers, *Fuel*, 2016, **173**, 129–137.
30 A. Bertola and K. Boulouchos, in *SAE Technical Paper Series*, SAE International400 Commonwealth Drive, Warrendale, PA, United States, 2000.

31 N. W. Boaz and B. Venepalli, Applications of Diethoxymethane as a Versatile Process Solvent and Unique Reagent in Organic Synthesis, *Org. Process Res. Dev.*, 2001, **5**, 127–131.
32 R. Ghorbani-Vaghei, M. A. Zolfigol, M. Amiri and H. Veisi, N,N,N′,N′ -Tetrabromobenzene-1,3-Disulfonamide and Poly(N -Bromo- N -Ethyl-Benzene-1,3-Disulfonamide) as Efficient Catalysts for the Methoxymethylation of Alcohols under Solvent-Free Conditions, *J. Chin. Chem. Soc.*, 2008, **55**, 632–635.
33 U.-A. Schaper, Die Einführung der O -Ethoxymethyl-Gruppe zum Schutz der Hydroxy-Gruppe in Alkoholen and Phenolen, *Synthesis*, 1981, **1981**, 794–796.
34 Symrise GmbH & Co. KG, *Deutschland Pat.*, DE10332229A1, 2003.
35 X. Luo, X. Ma, F. Lebreux, I. E. Markó and K. Lam, Electrochemical methoxymethylation of alcohols - a new, green and safe approach for the preparation of MOM ethers and other acetals, *Chem. Commun.*, 2018, **54**, 9969–9972.
36 D. L. Bartholet, M. A. Arellano-Treviño, F. L. Chan, S. Lucas, J. Zhu, P. C. St. John, T. L. Alleman, C. S. McEnally, L. D. Pfefferle, D. A. Ruddy, B. Windom, T. D. Foust and K. F. Reardon, Property predictions demonstrate that structural diversity can improve the performance of polyoxymethylene ethers as potential bio-based diesel fuels, *Fuel*, 2021, **295**, 120509.
37 S. Schemme, S. Meschede, M. Köller, R. C. Samsun, R. Peters and D. Stolten, Property Data Estimation for Hemiformals, Methylene Glycols and Polyoxymethylene Dimethyl Ethers and Process Optimization in Formaldehyde Synthesis, *Energies*, 2020, **13**, 3401.
38 F. Menges, *Spectragryph. optical spectroscopy software*, Dr Friedrich Menges Software-Entwicklung, 2020.
39 A. R. Katritzky, M. Kuanar, S. Slavov, C. D. Hall, M. Karelson, I. Kahn and D. A. Dobchev, Quantitative correlation of physical and chemical properties with chemical structure: utility for prediction, *Chem. Rev.*, 2010, **110**, 5714–5789.
40 D. A. Saldana, L. Starck, P. Mougin, B. Rousseau, L. Pidol, N. Jeuland and B. Creton, Flash Point and Cetane Number Predictions for Fuel Compounds Using Quantitative Structure Property Relationship (QSPR) Methods, *Energy Fuels*, 2011, **25**, 3900–3908.
41 S. Kaminski, E. Kirgios, A. Bardow and K. Leonhard, Improved Property Predictions by Combination of Predictive Models, *Ind. Eng. Chem. Res.*, 2017, **56**, 3098–3106.
42 L. S. Whitmore, R. W. Davis, R. L. McCormick, J. M. Gladden, B. A. Simmons, A. George and C. M. Hudson, BioCompoundML: A General Biofuel Property Screening Tool for Biological Molecules Using Random Forest Classifiers, *Energy Fuels*, 2016, **30**, 8410–8418.
43 M. Dahmen and W. Marquardt, Model-Based Design of Tailor-Made Biofuels, *Energy Fuels*, 2016, **30**, 1109–1134.
44 P. Gramatica, Principles of QSAR models validation: internal and external, *QSAR Comb. Sci.*, 2007, **26**, 694–701.
45 A. Golbraikh, M. Shen, Z. Xiao, Y.-D. Xiao, K.-H. Lee and A. Tropsha, Rational selection of training and test sets for the development of validated QSAR models, *J. Comput.-Aided Mol. Des.*, 2003, **17**, 241–253.
46 S. Weaver and M. P. Gleeson, The importance of the domain of applicability in QSAR modeling, *J. Mol. Graphics Modell.*, 2008, **26**, 1315–1326.
47 M. Dahmen and W. Marquardt, A Novel Group Contribution Method for the Prediction of the Derived Cetane Number of Oxygenated Hydrocarbons, *Energy Fuels*, 2015, **29**, 5781–5801.
48 K. G. Joback and R. C. Reid, Estimation of pure-component properties from group-contributions, *Chem. Eng. Commun.*, 1987, **57**, 233–243.
49 A. Alibakhshi, H. Mirshahvalad and S. Alibakhshi, Prediction of flash points of pure organic compounds: Evaluation of the DIPPR database, *Process Saf. Environ. Prot.*, 2017, **105**, 127–133.
50 S. Yan, E. G. Eddings, A. B. Palotas, R. J. Pugmire and A. F. Sarofim, Prediction of Sooting Tendency for Hydrocarbon Liquids in Diffusion Flames, *Energy Fuels*, 2005, **19**, 2408–2415.
51 X. Zhang and S. M. Sarathy, A functional-group-based approach to modeling real-fuel combustion chemistry – II: Kinetic model construction and validation, *Combust. Flame*, 2021, **227**, 510–525.
52 P. G. Seybold, M. May and U. A. Bagal, Molecular structure: Property relationships, *J. Chem. Educ.*, 1987, **64**, 575.
53 T. I. Netzeva, A. Worth, T. Aldenberg, R. Benigni, M. T. D. Cronin, P. Gramatica, J. S. Jaworska, S. Kahn, G. Klopman, C. A. Marchant, G. Myatt, N. Nikolova-Jeliazkova, G. Y. Patlewicz, R. Perkins, D. Roberts, T. Schultz, D. W. Stanton, J. J. M. van de Sandt, W. Tong, G. Veith and C. Yang, Current status of methods for defining the applicability domain of (quantitative) structure-activity relationships. The report and recommendations of ECVAM Workshop 52, *ATLA, Altern. Lab. Anim.*, 2005, **33**, 155–173.
54 S. S. Alqaheem and M. R. Riazi, Flash Points of Hydrocarbons and Petroleum Products: Prediction and Evaluation of Methods, *Energy Fuels*, 2017, **31**, 3578–3584.
55 K. Satyanarayana and P. G. Rao, Improved equation to estimate flash points of organic compounds, *J. Hazard. Mater.*, 1992, **32**, 81–85.
56 I. W. Mills, A. E. Hirschler and S. S. Kurtz, Molecular Weight-Physical Property Correlation for Petroleum Fractions, *Ind. Eng. Chem.*, 1946, **38**, 442–450.
57 R. M. Munavu, Conversion of alcohols to methylene acetals by reaction with dimethyl sulfoxide-bromine, *J. Org. Chem.*, 1980, **45**, 3341–3343.
58 B. I. Ionin and B. A. Ershov, in *NMR Spectroscopy in Organic Chemistry*, ed. B. I. Ionin and B. A. Ershov, Springer, Boston, MA, 1995, pp. 1–59.
59 D. Lin-Vien, N. B. Colthup, W. G. Fateley and J. G. Grasselli, *The Handbook of Infrared and Raman Characteristic Frequencies of Organic Molecules*, Academic Press, Boston, 1991.

60 Spectral data were obtained from Wiley Subscription Services, Inc. (US), ID_WID-DLO-005807-1, accessed 9 April 2021.
61 Data were obtained from the National Institute of Advanced Industrial Science and Technology (Japan) (AIST: Integrated Spectral Database System of Organic Compounds), MS-NW-5531 SDBS NO. 792, accessed 9 April 2021.
62 Spectral data were obtained from Wiley Subscription Services, Inc. (US), ID_WID-DLO-012761-7, accessed 9 April 2021.
63 C. R. Noller, *Chemistry of Organic Compounds*, W. B. Saunders Company, 3rd edn, 1966.
64 K. Mollenhauer and H. Tschöke, *Handbuch Dieselmotoren*, Springer Verlag, Berlin, Heidelberg, 2007.
65 W.-Q. Han and C.-D. Yao, Research on high cetane and high octane number fuels and the mechanism for their common oxidation and auto-ignition, *Fuel*, 2015, **150**, 29–40.
66 S. K. Hoekman, A. Broch, C. Robbins, E. Ceniceros and M. Natarajan, Review of biodiesel composition, properties, and specifications, *Renewable Sustainable Energy Rev.*, 2012, **16**, 143–169.
67 G. Knothe, in *SAE Technical Paper Series*, SAE International400 Commonwealth Drive, Warrendale, PA, United States, 2005.
68 E. Jacob, M. Stark, M. Härtl and G. Wachtmeister, in *11. Tagung Einspritzung und Kraftstoffe 2018*, ed. H. Tschöke and R. Marohn, Springer Vieweg, Wiesbaden, 2019, pp. 17–55.
69 T. Wilharm, H. Stein and I. Bogatykh, in *Internationaler Motorenkongress 2020*, ed. J. Liebl, C. Beidland W. Maus, Springer Vieweg, Wiesbaden, 2020, pp. 205–211.
70 Y. Ren, Z. Huang, H. Miao, Y. Di, D. Jiang, K. Zeng, B. Liu and X. Wang, Combustion and emissions of a DI diesel engine fuelled with diesel-oxygenate blends, *Fuel*, 2008, **87**, 2691–2697.
71 M. Ghysels, Contribution à l'étude des formals des alcools primaires, *Bull. Soc. Chim. Belg.*, 1924, **33**, 57–78.
72 P. Zheng, X. Meng, J. Wu and Z. Liu, Density and Viscosity Measurements of Dimethoxymethane and 1,2-Dimethoxyethane from 243 K to 373 K up to 20 MPa, *Int. J. Thermophys.*, 2008, **29**, 1244–1256.
73 D. R. Lide, *CRC Handbook of Chemistry and Physics*, Taylor & Francis, 93rd edn, 2012.
74 G. Knothe, A. C. Matheaus and T. W. Ryan, Cetane numbers of branched and straight-chain fatty esters determined in an ignition quality tester☆, *Fuel*, 2003, **82**, 971–975.
75 S. M. Heck, H. O. Pritchard and J. F. Griffiths, Cetane number vs. structure in paraffin hydrocarbons, *J. Chem. Soc., Faraday Trans.*, 1998, **94**, 1725–1727.
76 G. Sivaraman, N. E. Jackson, B. Sanchez-Lengeling, Á. Vázquez-Mayagoitia, A. Aspuru-Guzik, V. Vishwanath and J. J. de Pablo, A machine learning workflow for molecular analysis: application to melting points, *Machine Learning: Science and Technology*, 2020, **1**, 25015.
77 A. M. Schweidtmann, J. G. Rittig, A. König, M. Grohe, A. Mitsos and M. Dahmen, Graph Neural Networks for Prediction of Fuel Ignition Quality, *Energy Fuels*, 2020, **34**, 11395–11407.

